

***DEACTIVATION, REACTIVATION AND MEMORY EFFECT ON Co-B  
CATALYST FOR SODIUM BOROHYDRIDE HYDROLYSIS OPERATING IN  
HIGH CONVERSION CONDITIONS***

G.M. Arzac<sup>1\*</sup>, D. Hufschmidt<sup>1</sup>, M.C. Jiménez De Haro<sup>1</sup>, A. Fernández<sup>1</sup>, B. Sarmiento<sup>2</sup>,  
M.A. Jiménez<sup>2</sup>, M.M. Jiménez<sup>2</sup>

<sup>1</sup> Instituto de Ciencia de Materiales de Sevilla, CSIC-Univ. Sevilla, Américo Vespucio  
49, Isla de la Cartuja, Seville, Spain.

<sup>2</sup> Abengoa Hidrógeno, S.A., Campus Palmas Altas, Seville, Spain

\* Corresponding author: phone number: +34954489552, fax number: +34954460665, e-  
mail: gisela@icmse.csic.es

**Abstract**

A system with a continuous reactor to produce hydrogen by sodium borohydride hydrolysis was designed and built. The purpose was to test a supported Co-B catalyst durability upon cycling and long life experiments in high conversion conditions. A Stainless Steel monolith was built and calcined to improve adherence. For comparison a Ru-B catalyst was tested upon cycling. Both Co-B and Ru-B catalysts are durable during 6 cycles and then deactivate. A known reactivation procedure has proven to be more effective for the Co-B than for the Ru-B catalyst. This is related to stronger adsorption of B-O based compounds on the Co-B catalyst which is reversible upon acid washing. For the Ru-B catalyst deactivation may be more related to particle agglomeration than to the adsorption of B-O based species. The continuous system enlarges the catalysts durability because of the continuous borate elimination at elevated temperatures.

## Keywords

*Hydrogen production, sodium borohydride, continuous reactor, S.S. supported Co-B catalyst, high conversion, deactivation.*

## 1. Introduction

Sodium borohydride (NaBH<sub>4</sub>, SBH) hydrolysis is a high-potential method to store and produce hydrogen for portable applications. Since SBH is a high-hydrogen content hydride reaction (1) is advantageous because of being safe, controllable and due to its exothermic character being spontaneous and self-maintaining [1, 2].



For this reaction to produce hydrogen at appreciable rates, it is necessary the addition of catalysts. Lowering the solution pH or adding metal based catalysts are the two methods that Scheslinger et al identified many years ago [3]. Following this work and mainly in the past decade the studies on the catalytic (powder or supported metal based catalysts) and non- catalytic (high temperature steam, addition of acid, etc) hydrogen release through reaction (1) were reported [1-2, 4]. Among metal based catalysts, cobalt and nickel have been the most investigated among non-noble metals and ruthenium and platinum the most reported between the noble metals [1-2, 4-6]. Co-B materials are the most investigated cobalt based catalysts and have been prepared on a wide range of conditions in powder as well as in supported form [4-6]. To the best of our knowledge, up to now most investigations have focused on the development of new metal based

catalysts and/or new supports, but only a few have intended to conduct tests to determine their cycling stability [4]. Very recently it was reported a study on the durability of a Cobalt based catalyst in conditions to produce up to  $\sim 125 \text{ ml} \cdot \text{min}^{-1}$  hydrogen during a few minutes [7].

Herein we present a work in which durability of a Co-B based catalyst is evaluated in conditions that approach to a “real” application, which operates in high SBH conversion conditions. A reactor was designed and built as a part of a system to produce hydrogen from reaction (1) through the controlled addition of SBH fuel solutions to a supported catalyst. This system was thought to be multi-use. We chose a concentrated (19 wt %) SBH fuel solution because of its high gravimetric potential [8]. The fuel addition rate was selected to produce  $0.8\text{-}1.2 \text{ L} \cdot \text{min}^{-1}$  hydrogen. Temperatures of  $100\text{-}120^\circ\text{C}$  were achieved. The supported catalyst is a Co-B based material and it was prepared by chemical methods for the first time on bare and oxidized Stainless Steel (SS) home made monoliths searching for high adherence and contact with the fuel solution. Adherence was tested during 60 minutes-long-experiments. Durability of supported Co-B catalyst was tested by repeating the previous experiment for 11 cycles. Long life experiments were performed during 9 hours of hydrogen production. To compare the results a supported Ru-B catalyst was prepared for the first time on a previously oxidized SS monolith and durability was also tested during 11 cycles. Previously reported reactivation steps were used in this work when necessary and the effect of these steps assessed [7, 9].

Deactivation and reactivation is discussed herein in terms of formation, accumulation and elimination of B-O species, memory effect and nanoparticle growth.

## **2. Experimental**

### **2.1. The continuous system and the reactor**

For the experiments a home made system was designed and built [10]. Figure 1.a. shows a scheme of the system. It consists of a PP storage containing the stabilized fuel solution, which is connected with a commercial membrane pump. The cylindrical reactor is made of PMMA with a total volume of 11 mL (Fig.1.b). The reaction gas-liquid mixture flows from the reactor into a tank, which serves as a gas-liquid separator and in parallel provides a recipient volume for the residues. The hydrogen gas stream was further dried and purified by installing a 250 mL PP bottle filled with dry silica-gel. Hydrogen gas flow was measured by a flowmeter (Bronkhorst MassView MV-394-H2). The temperature at the exit of the reactor was measured by a thermocouple. The hydrogen generation rate (HGR) was constantly monitored as a function on time with the flowmeter connected to a PC. From the experiments, an (avgHGR $\pm$  error) (average Hydrogen Generation Rate) is obtained graphically from the HGR vs time plot, including the maximum fluctuations in the experimental error. The total conversion (TC %) was calculated as  $100 \times V/V_{th}$  where V represents the product between the avg HGR and the time (avgHGR x time) and  $V_{th}$  was calculated as the theoretical volume of hydrogen (at room temperature) to be obtained from the total volume of 19wt% fuel solution.

## 2.2. Support preparation

As catalyst support homemade monoliths made from commercially available perforated stainless steel (SS316) were employed [10]. After washing in an ultrasound bath for 20 min using first deionised water and then 20 min using acetone to remove inorganic and organic impurities the thus obtained supports were weighted. The SS support was calcined at 900°C [10]. The adherence of the produced oxide layer was tested by immersing in an ultrasonic bath 20 minutes in deionized water and 20 minutes in acetone. The monolith was weighed before and after sonication and the loss of weight was calculated. No loss of the oxide layer was found for the calcined monolith.

## **2.3. Catalysts**

### **2.3.1 Catalysts preparation**

Two techniques were employed in this work and they are described as following:

i)  $\text{Co}_{\text{aq}}/\text{SBH}_{\text{aq}}$  technique has been used to prepare the Co-B catalyst on bare SS monoliths. The technique was used before and consists of 12 cycles of alternate immersions of the support on 30%  $\text{CoCl}_2 \cdot 6\text{H}_2\text{O}$  aqueous solution and on a stabilized 19 wt% SBH aqueous solution [8].

ii) The  $\text{Co}_{\text{ETOH}}$  or  $\text{Ru}_{\text{ETOH}}/\text{SBH}_{\text{aq}}$  technique similar to the one described in i) was employed to prepare the Co-B and Ru-B catalysts on previously oxidized SS monoliths. It is based on the use of ethanolic 30%  $\text{CoCl}_2 \cdot 6\text{H}_2\text{O}$  or  $\text{RuCl}_3 \cdot 3\text{H}_2\text{O}$  solutions as metal source [10]. After preparation, all samples were then treated at 573 K (heating rate  $1^\circ\text{C}/\text{min}$ ) in pure Helium environment for 2h before cooling to room temperature.

### **2.3.2 Catalysts characterization**

For characterization catalysts were also prepared on  $900^\circ\text{C}$  calcined 316 SS sheets (1cmx1cm). The sheets were also included in the reactor in all experiments and extracted for characterization. X-ray diffraction measurements were performed using  $\text{Cu K}\alpha$  radiation in a Siemens D5000 diffractometer in a Bragg-Brentano configuration in the  $2\theta$  angle range of 40-80 degrees.

Scanning electron microscopy (SEM) was performed to study the morphology of samples in a high resolution FEG microscope, HITACHI S4800.

### **2.3.3 Catalysts adherence and durability tests**

As it was desired to approach the study to real conditions, adherence and durability (upon cycles and in long term experiments) were tested in conditions of intense hydrogen bubbling at high temperatures.

The tests were conducted on the system described in 2.1 under a  $2.8\text{ml}\cdot\text{min}^{-1}$  constant flow of a fresh 19 wt % SBH solution stabilized in 4.5 wt % NaOH on the selected supported fresh catalyst. The fuel addition rate was selected to produce  $0.8\text{-}1.2\text{ L}\cdot\text{min}^{-1}$   $\text{H}_2$  which results in a temperature of  $100\text{-}120\text{ }^\circ\text{C}$ . The system was kept working during 60 min for the adherence and durability cycles tests and 9 hours during the long life tests. Then the fuel addition was interrupted. The reactor was allowed to reach room temperature, and then monoliths were extracted, washed with water and ethanol and dried under  $\text{N}_2$  flow.

The monoliths were weighted before and after operation and then the catalyst loss was calculated.

### **3. Results and Discussion**

#### **3.1. SS and oxidized SS support**

It is known that calcination of stainless steel produces an oxide layer that increases surface roughness and consequently the adhesion of catalysts [11-12]. For this reason Co-B catalyst was prepared using non-treated (bare) and oxidized SS monoliths [10]. Figure 2.a includes a SEM image of a non-treated SS monolith in comparison to a calcined SS monolith (Fig.2.b). Fig 2c. and 2.d. show the fresh Co-B prepared on both monoliths respectively. The surface roughness of the oxidized monolith induces a high degree of porosity at constant catalyst load ( in the range of  $10\text{-}14\text{ mg}_{\text{cat}}\text{g}_{\text{support}}^{-1}$  for bare and for the previously oxidized SS monolith). Adherence of Co-B catalyst supported on bare and oxidized SS monolith was 90% and 100% respectively (in both cases, tests conducted in duplicate). In the following sections Co-B catalyst will be supported on the previously oxidized monolith.

#### **3.2. Study of the reactor behaviour.**

The exothermic character of reaction (1) makes heat management a key issue. In this reactor the heat released in the reaction has to compensate heat losses due to heating-up of the fuel, heat transport out of the reactor by the reaction products and heat losses of the reactor to the surrounding. The heat production of the employed fuel and the chosen flow rate was sufficient to initiate and maintain the reaction. Figure 3.a. shows that for a selected fuel addition rate steady state with a constant HGR (avgHGR equal to  $0.9 \text{ L} \cdot \text{min}^{-1}$ ) and constant temperature ( $103^\circ\text{C}$ ) are obtained [10]. With this reactor it is possible to obtain stable hydrogen generation in the range of  $1.66\text{-}0.3 \text{ L} \cdot \text{min}^{-1}$  at constant temperatures (above the melting point of sodium borates) by varying the fuel addition rate [10]. For HGR lower than  $0.3 \text{ L} \cdot \text{min}^{-1}$  heat production is not sufficient to achieve appropriate temperature for the reactor maintain stable hydrogen generation. Lower HGRs would require an adapted reactor design.

When conducting durability experiments, a decrease in hydrogen generation rate could not only be attributed to a deactivation of the catalyst but also to the loss of catalyst during operation. To evaluate the effect of the amount of supported Co-B in the hydrogen generation rate, a series of previously calcined monoliths were prepared with variable catalyst amount. These catalysts were tested in the reactor at  $2.8 \text{ ml} \cdot \text{min}^{-1}$  fuel addition rate.

Figure 4 and table 1 show that Co-B load ( $\text{mg}_{\text{cat}} \cdot \text{g}_{\text{support}}^{-1}$ ) increases linearly with the number of coatings. The avg HGR responds sigmoidal to the mass of catalyst. With low catalyst amounts (7 mg) the reaction rate is not high enough to reach an appropriate temperature to self-maintain the hydrogen production. At 37 mg Co-B the reactor produces enough hydrogen and heat to achieve a  $0.8 \text{ L} \cdot \text{min}^{-1}$  hydrogen production at  $\sim 100^\circ \text{C}$ . An increase in the catalyst load does not cause significant variations in the hydrogen generation rate. This suggest that when the catalyst load is higher than 7mg hydrogen generation rate is determined by the fuel addition rate and not by catalytic

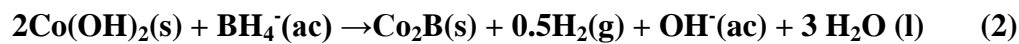
activity of the catalyst, except the deactivation achieves a degree that the reaction rate becomes catalyst-determined. The activity of the catalyst can be calculated as  $27 \text{ L}_{\text{hydrogen}} \cdot \text{min}^{-1} \cdot \text{g}_{\text{catalyst}}^{-1}$  which is between the highest ever reported activities for a non noble catalyst and means that oxidized monolith is a good dispersant [4].

This behaviour is useful when studying the deactivation process, since a significant reduction of the hydrogen generation rate can be definitely attributed to a deactivation process on condition that the catalyst loss is not high enough.

### 3.3. Durability of Co-B and Ru-B catalysts upon cycling

#### 3.3.1. Co-B catalyst

A fresh Co-B catalyst was tested in the continuous reactor at a  $2.8 \text{ ml min}^{-1}$  fuel addition rate during 60 min during 11 start-and-stop reuse cycles. Except for cycle 3, the reaction was initiated with a first addition of a small amount of fuel and waiting until the temperature reached at least  $60^\circ \text{ C}$ . This step represents an *in situ* reactivation (2) [8-9].



After 60 min of operation the reaction was interrupted, the monolith was washed with water and then with ethanol and dried at open air. After weighing of the monolith for the determination of catalyst losses the monolith was reused in additional 60 min cycles. The results of these experimental run are shown in Table 2. Figure 5.b represents the variation of the normalized avgHGR as a function of the number of cycle. A slight decrease of the normalized avg HGR was observed in the second cycle. However successive repetitions do not present any significant variations of the avgHGR until in cycle 7 a complete deactivation of the catalyst was observed. In this cycle at the beginning a slightly lower activity was observed, which dropped rapidly after ca. 10 min of reaction time to zero (Fig.5a). Repetition of this experiment confirmed this



result. In previous papers a layer of B-O based species on the catalyst surface were identified as being responsible of the deactivation of Co catalysts [7, 13]. Based on this assumption a reactivation step was applied, which consisted in washing with diluted acid solution to eliminate B-O based compounds on the surface similarly to reference [7]. After this reactivation step the avgHGR recovered in the subsequent cycles 9, 10 and 11. Nevertheless even by acidic treatment the avgHGR did not reach fully the initial value ( $\text{avgHGR}_0$ ), which indicates that more stable and resistant B-O based species were formed and/or that some more profound change of the catalyst has taken place.

Figure 6 shows SEM micrographs for the fresh Co-B catalyst (6.a-b) in comparison to the catalyst before reactivation (6.c-d) and the diluted acid reactivated (5.f-g) Co-B. The fresh catalyst (Fig.6.a) is very porous and higher magnification micrographs clearly show the formation of spherical nanoparticles (Fig.6.b). Fig 6.c. shows the catalyst before acid reactivation. It seems to have lost porosity and dispersion, which could indicate a deposition of B-O based species on the catalyst surface. High magnification (Fig.6.d.) shows the same layer that was previously recognized as the B-O based deactivating network [7]. After diluted acid reactivation, the structure of the catalyst seems to be recovered from a textural point of view (Fig.6.f.), but porosity is still lower than in the case of the fresh catalyst (Fig.6.a.). This could explain that the activity is recovered after diluted acid treatment but not to the same extent than in the 1-6 cycles. It seems that B-O based species are formed on the catalyst surface, which could not be removed fully by diluted acid treatment but remain partially. Higher magnification (6.g.) supports this assumption showing that the nanoparticles are accessible again but part of the catalyst is still covered by the B-O species' layer.

Except for cycle 3 adherence of the catalyst during the 11 cycles was found to be as high on condition that the *in situ* reactivation was performed. Neither visible loss of catalyst was observed nor was Co-B powder found in the residual tank.

### 3.3.2. Supported Ru-B as catalyst

Previous studies suggested that Ru based catalysts could be more stable against deactivation [14, 15]. To prove this we prepared a Ru-B catalyst on a previously oxidized monolith and we tested it upon cycling in the same conditions than the Co-B catalyst [10]. In the first 7 cycles we found a behaviour similar to that of the Co-B catalyst (section 3.3.1). During the first three cycles the avgHGR of the Ru-B remained constant. In the following cycles 4-6 a slight drop of avgHGR was observed (90% of avgHGR retained in respect to the initial) until in cycle 7 a complete deactivation occurred (Fig.7). Diluted acid washing as reactivation step permits to recover the avgHGR in a single cycle but in subsequent cycles deactivation again is observed. After a second reactivation avgHGR diminished to a 60% in respect to the initial and finally deactivated completely for a third time. Figure 8.a. shows a representative SEM image of the fresh Ru-B catalyst in comparison to the deactivated catalyst (Fig.8.b.) after 11 cycles. In this case B-O based species' formation seems not to be the critical effect but evidence of particle aggregation is found in SEM images of the deactivated catalyst. On the other hand the catalyst treated with diluted acid showed in studies by SEM no microstructural difference in respect to the deactivated one despite avgHGR is partly recovered. This supports the assumption that deactivation is depending on formation of B-O based compounds on one side and on the other side on particle agglomeration but in this case the latter is the determining effect.

### 3.4. Durability of the Co-B catalyst in a long-life experiment.

A long time continuous experiment (9h) was conducted on a fresh Co-B catalyst on oxidized SS monolith. Stable hydrogen generation at the same HGR was obtained during 4 hours and then HGR decreased slowly to reach 90% of the initial at the end of

the experiment (Figure 9). The catalyst is clearly more durable in a single long time experiment than upon start-stop cycling. SEM micrographs of the fresh Co-B catalyst (Fig. 10.a-b) in comparison to the 9h used Co-B (Fig. 10.c-d) show that the formation of B-O compounds is here not occurring and no evidence of particle aggregation is found. The catalyst used continuously of 9 hours is as disperse and porous as the fresh. XRD measurements show that the continuously used catalyst presents a broad peak between 20-45 2θ degrees with some sharp peaks which were identified as coming from a Na<sub>2</sub>B<sub>4</sub>O<sub>7</sub> layer (Fig 11, indicated by arrows) . Adherence of the Co-B catalyst was higher for the 9h experiment than for the 9 cycle experiments.

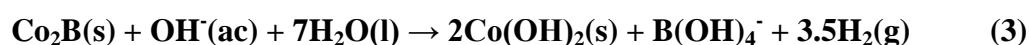
Diluted acid washing was successful in removing this Na<sub>2</sub>B<sub>4</sub>O<sub>7</sub> layer but also is aggressive with the catalyst because it destroys its adherence. It is concluded that the formation of B-O based compounds network could be the responsible of the 10% loss of *avgHGR respect to the initial*.

Based on these observations it can be concluded that the formation of borates on the catalyst surface, which is responsible for the loss of activity and adherence together with the intense hydrogen formation of the catalytic layer, mostly is occurring during the start or stop operations. On the other side the conditions under which the reaction is taking place inside the reactor is mostly inhibiting this formation of B-O species on the catalyst surface and are extending largely the life time and stability of the supported catalyst.

### **3.5. Deactivation, reactivation step and memory effect.**

Three deactivation mechanisms of the catalyst for reaction (1) have been reported [4,7, 9, 13]

- i) Oxidation of the Co catalyst at the end of the reaction as suggested in equation (3) [9].



- ii) Accumulation of B-O and (Na,Co) based compounds on the catalyst surface [7,13]
- iii) Agglomeration of particles [13].

The strong alkaline medium also favours catalysts deactivation and this effect cannot be disregarded.

Deactivation by mechanism i) should be recovered by a treatment with a reducing agent, which in our case is the fuel solution itself. The *in situ* treatment applied in our work was able to recover the catalytic activity of the Co-B and the Ru-B catalyst at least partially. A washing of the catalyst with a diluted acidic solution is expected to be efficient against deactivation by mechanism ii). The *ex situ* reactivation by acidic solution showed mostly good results in the case of the Co-B catalyst upon cycling, in which SEM has shown a strong B-O based compounds formation (Fig 7 c-d). In the case of the Ru-B catalyst a much lower B-O species formation was observed, but also *in situ* and *ex situ* reactivations proved to be much less efficient. In this case a deactivation by particle aggregation according to mechanism iii) seems to take place (Fig 9).

Long life of the Co-B catalyst is affected mainly by B-O species formation and no aggregation was found. In this case B-O species based network is not as strong as in cycling experiments which explains the high durability and no deactivation after 6 h use. The start-stop, washing, cooling and storing of the catalyst seems to stabilize the B-O species' layer with a higher deactivation effect. Because of the sigmoid reactor behaviour (section 3.2.) B-O based compounds' accumulation does not produce a significant effect until the catalyst surface is highly covered. *Ex situ* diluted acid reactivation was not completely effective and is negative for catalyst adherence. On the contrary, high temperature reaction and B-O based compounds' elimination in the continuous system makes the catalyst more durable on long experiments.

Very recently it was reported the absorption of small amounts of hydrogen on catalysts during preparation processes [16]. This may result in metal catalyst pulverization due to the effect of lattice expansion. Despite it should be further studied, this effect cannot be disregarded in herein presented experiments, not only during catalyst preparation but also during each start-stop cycle.

#### **4. Conclusions**

The intention of this work was to explore the performance of a Co-B catalyst for the production of hydrogen by SBH hydrolysis under conditions of a practical use. This included a continuous long time use of the catalyst and a high throughput of SBH to achieve a high hydrogen production rate. For this purpose a system was designed including a continuous reactor and the catalyst supported on a SS monolith. To the best of our knowledge it is the first time that a Co-B catalyst is prepared on a previously calcined SS monolith, which has proven to be a good catalyst dispersant, cheap and adherent enough to conduct cycling and long time experiments. Special interest was laid on long time **durability** of the catalyst and on possibilities to regenerate the catalyst in order to recover its activity. In long time experiments the continuous system showed the possibility of using the synergies between operational temperature and continuous elimination of borates formed in the reaction. A certain deactivation of the catalyst was observed. Two kinds of reactivation techniques were applied, an *in situ* reactivation step consisting in a pre-treatment by SBH and an *ex situ* step by washing with a diluted acid solution, which were able to restore mostly the catalyst activity. Nevertheless, a deactivation after several cycles in a start-stop operational mode could be observed, which proved to be resistant to intents of regeneration. This memory effect can be related to the formation of a network B-O based compounds on the Co-B surface. Co-B particle aggregation seems no to be a major deactivation process neither for long time

continuous nor for cycling experiments. In the case of and Ru-B catalyst particle agglomeration seems to be the major deactivation process but the formation of surface borates cannot be disregarded.

M-B chemistry is put in evidence here. In the case of the Co-B material metal metalloids interactions, which are highly stabilizing particles against agglomeration, B-O adsorption is higher but reversible upon acid washing [15-17]. In the case of the Ru-B material the low affinity of ruthenium to boron makes the catalyst more susceptible to particle agglomeration and prevents B-O adsorption making washing with acids less effective [15]. The study of particle aggregation will be conducted in a further study through TEM (Transmission Electron Microscopy) and HREM (High Resolution Electron Microscopy).

In this work was demonstrated that in practical uses for a high rate Hydrogen production non noble catalysts like Co are presenting very good and cheap alternatives to noble metal catalysts.

### **Acknowledgements**

Financial support from Abengoa Hidrógeno S.A., MICINN (Project CTQ2009-13440), “Junta de Andalucía” (TEP217) and the EC (CT-REGPOT-2011-1-285895, AL-NANOFUNC) is acknowledged.

We thank to Dr. Angel Justo for the XRD measurements.



## 5. References

- [1] B.H. Liu, Z.P. Li. A review: Hydrogen generation from borohydride hydrolysis reaction. *J. Power Sources*, 2009; 187: 527-534. References therein
- [2] U.B Demirci, O.Akdim, J. Andrieux, J. Hannauer, R. Chamoun, P.Miele. Sodium borohydride hydrolysis as hydrogen generator: Issues, state of the art and applicability upstream from a Fuel Cell. *Fuel Cells*, 2010; 3: 335-350. References therein
- [3] H.I. Schlesinger, H.C. Brown, A.E. Finholt, J.R. Gilbreath, H.R. Hoekstra, E.K. Hyde. Sodium borohydride, its hydrolysis and its use as a reducing agent and in the generation of hydrogen. *J. Am. Chem. Soc.*, 1953; 75: 215-219.
- [4] S.S. Muir, X. Yao, Progress in sodium borohydride as a hydrogen storage material: Development of hydrolysis catalysts and reaction systems. *Int J. Hydrogen Energy*, 2011; 36: 5983-5997. References therein
- [5] U.B. Demirci, P.Miele, Cobalt in  $\text{NaBH}_4$  hydrolysis. *Phys. Chem. Chem Phys*, 2010; 12: 14665-14651. References therein
- [6] U.B. Demirci, O. Akdim, J. Hannauer, R. Chaumoun, P. Miele. Cobalt, a reactive metal in releasing hydrogen from sodium borohydride by hydrolysis: A short review and a research perspective. *Sci China Chem*, 2010; 53: 1870-1879.
- [7] O.Akdim, U.B. Demirci, P. Miele, Deactivation and reactivation of cobalt in hydrolysis of sodium borohydride. *Int. J. Hydrogen Energy*, 2011; 36: 13669-13675.
- [8] G.M. Arzac, A. Fernández, A. Justo, B. Sarmiento, M.A. Jiménez, M.M. Jiménez. Optimized hydrogen generation in a semicontinuos sodium borohydride hydrolysis reactor for a 60-W scale fuel cell stack. *Journal of Power Sources*, 2011; 196: 4388-4395
- [9] A. Garron, D. Świerczyński, S. Bennici, A. Auroux. New insights into the mechanism of  $\text{H}_2$  generation through  $\text{NaBH}_4$  hydrolysis on Co-based nanocatalysts



studied by differential reaction calorimetry. *Int. J. Hydrogen Energy*, 2009; 34: 1185-1199.

[10] G.M. Arzac, D. Hufschmidt, E Jiménez Roca, A. Fernández, M.A. Jiménez, S. Tyagi, M.M. Jiménez, B. Sarmiento. "Proceso de producción de hidrógeno mediante hidrólisis catalítica en un reactor continuo para llevar a cabo dicho procedimiento". Spanish patent application: P201230221. Priority date: 14-Feb-2012. Presented by Abengoa Hidrógeno S.A.

[11] J.P. Bortolozzi, E.D. Banús, V.G. Milt, L.B. Gutierrez, M.A. Ulla. The significance of passivation treatments on AISI 314 foam pieces to be used as substrates for catalytic applications. *App. Surf. Sci*, 2010; 257: 495-502.

[12] P. Avila, M. Montes, E.E. Miró, Monolithic reactors for environmental applications A review on preparation technologies. *Chem. Eng. Journal*, 2005; 109: 11-36.

[13] J.H. Kim, K.T. Kim, Y.M. Kang, H.S. Kim, M.S. Song, Y.J.Lee, P.S.Lee, J.Y. Lee, Study on degradation of filamentary Ni catalyst on hydrolysis of sodium borohydride. *J.Alloys and Compds.*, 2004; 379: 222-227.

[14] U.B. Demirci, F. Garin, Ru-based bimetallic alloys for hydrogen generation by hydrolysis of sodium tetrahydroborate, *J. Alloys and Compds*, 2008; 463: 101-111

[15] G.M. Arzac, T.C. Rojas, A. Fernández, New insights into the synergistic effect in bimetallic-boron catalysts for hydrogen generation: The Co-Ru-B system as a case study. <http://dx.doi.org/10.1016/j.apcatb.2012.02.013>

[16]H.B. Dai, Y. Liang, P. Wang, Effect of trapped hydrogen on the induction period of cobalt-tungsten-boron/nickel foam catalyst in catalytic hydrolysis reaction of sodium borohydride. *Catalysis Today*, 2011; 170, 27-32.

[17] G.M. Arzac, T.C. Rojas, A. Fernández, Boron compounds as stabilizers of a complex microstructure in a Co-B catalyst for NaBH<sub>4</sub> hydrolysis. *Chem Cat Chem*, 2011; 3: 1305-1313.



## Figure captions

**Figure 1.** (a) Scheme of the home made system: (1) fuel tank, (2) pump, (3) continuous reactor (4) separation tank (5) drying system (6) flowmeter and (7) thermocouple  
(b) Scheme of the continuous reactor.

**Figure 2.** SEM micrographs of the SS. Monolith (a) before and (b) after calcination at 900°C. SEM micrographs of the fresh Co-B catalyst prepared on (c) bare SS monolith and on a (d) 900° C calcined SS monolith.

**Figure 3.** (a) Hydrogen Generation Rate and temperature as a function of time for 2.8ml.min<sup>-1</sup> fuel addition rate on a fresh Co-B catalyst.

**Figure 4.** Average Hydrogen Generation Rate under fixed fuel addition rate in employing the continuous reactor and Co-B catalyst load as a function of the number of coatings.

**Figure 5.** (a) Hydrogen Generation Rate as a function of time for the first, the seventh and the ninth (after diluted acid reactivation) cycle on the same Co-B supported catalyst.  
(b) Catalytic activity represented by the normalized rate ( $\text{avgHGR}/\text{avgHGR}_0$  where  $\text{avgHGR}_0$  represents the average HGR for cycle 1) as a function of the cycle number for the cycling experiments on supported Co-B catalyst.

**Figure 6.** SEM micrographs at two different magnifications of the Co-B catalyst upon cycling at different stages: (a-b) Fresh catalyst (c-d) the Co-B catalyst used 8 times; before diluted acid reactivation ; (f-g) the Co-B catalyst after diluted acid reactivation.

**Figure 7.** Catalytic activity represented by the normalized rate ( $\text{avgHGR}/\text{avgHGR}_0$ , where  $\text{avgHGR}_0$  represents the average HGR for cycle 1) as a function of the cycle number for the supported Ru-B catalyst for the start-stop experiments.

**Figure 8.** SEM micrographs of the **(a)** fresh and **(b)** the deactivated ( after 11 cycles) Ru-B supported catalyst.

**Figure 9.** Hydrogen Generation Rate as a function of time for the 9h long life test on a fresh supported Co-B catalyst.

**Figure 10.** SEM micrographs of the fresh **(a-b)** and the 9h continuously used **(c-d)** Co-B catalyst.

**Figure 11.** XRD of the fresh Co-B catalyst in comparison to the 9h continuously used after and before diluted acid reactivation. The substrate diffractogram is also included.

## Table Legends

**Table 1.** Average HGR and catalyst load as a function of the number of Co-B coatings.

**Table 2.** Experimental parameters for the 11 cycle experiment on the Co-B catalyst.

***DEACTIVATION, REACTIVATION AND MEMORY EFFECT ON Co-B  
CATALYST FOR SODIUM BOROHYDRIDE HYDROLYSIS OPERATING IN  
HIGH CONVERSION CONDITIONS***

G.M. Arzac<sup>1\*</sup>, D. Hufschmidt<sup>1</sup>, M.C. Jiménez De Haro<sup>1</sup>, A. Fernández<sup>1</sup>, B. Sarmiento<sup>2</sup>,  
M.A. Jiménez<sup>2</sup>, M.M. Jiménez<sup>2</sup>

<sup>1</sup> Instituto de Ciencia de Materiales de Sevilla, CSIC-Univ. Sevilla, Américo Vespucio  
49, Isla de la Cartuja, Seville, Spain.

<sup>2</sup> Abengoa Hidrógeno, S.A., Campus Palmas Altas, Seville, Spain

\* Corresponding author: phone number: +34954489552, fax number: +34954460665, e-  
mail: gisela@icmse.csic.es

**Abstract**

A system with a continuous reactor to produce hydrogen by sodium borohydride hydrolysis was designed and built. The purpose was to test a supported Co-B catalyst durability upon cycling and long life experiments in high conversion conditions. A Stainless Steel monolith was built and calcined to improve adherence. For comparison a Ru-B catalyst was tested upon cycling. Both Co-B and Ru-B catalysts are durable during 6 cycles and then deactivate. A known reactivation procedure has proven to be more effective for the Co-B than for the Ru-B catalyst. This is related to stronger adsorption of B-O based compounds on the Co-B catalyst which is reversible upon acid washing. For the Ru-B catalyst deactivation may be more related to particle agglomeration than to the adsorption of B-O based species. The continuous system enlarges the catalysts durability because of the continuous borate elimination at elevated temperatures.

## Keywords

*Hydrogen production, sodium borohydride, continuous reactor, S.S. supported Co-B catalyst, high conversion, deactivation.*

## 1. Introduction

Sodium borohydride (NaBH<sub>4</sub>, SBH) hydrolysis is a high-potential method to store and produce hydrogen for portable applications. Since SBH is a high-hydrogen content hydride reaction (1) is advantageous because of being safe, controllable and due to its exothermic character being spontaneous and self-maintaining [1, 2].



For this reaction to produce hydrogen at appreciable rates, it is necessary the addition of catalysts. Lowering the solution pH or adding metal based catalysts are the two methods that Scheslinger et al identified many years ago [3]. Following this work and mainly in the past decade the studies on the catalytic (powder or supported metal based catalysts) and non- catalytic (high temperature steam, addition of acid, etc) hydrogen release through reaction (1) were reported [1-2, 4]. Among metal based catalysts, cobalt and nickel have been the most investigated among non-noble metals and ruthenium and platinum the most reported between the noble metals [1-2, 4-6]. Co-B materials are the most investigated cobalt based catalysts and have been prepared on a wide range of conditions in powder as well as in supported form [4-6]. To the best of our knowledge, up to now most investigations have focused on the development of new metal based

catalysts and/or new supports, but only a few have intended to conduct tests to determine their cycling stability [4]. Very recently it was reported a study on the durability of a Cobalt based catalyst in conditions to produce up to  $\sim 125 \text{ ml} \cdot \text{min}^{-1}$  hydrogen during a few minutes [7].

Herein we present a work in which durability of a Co-B based catalyst is evaluated in conditions that approach to a “real” application, which operates in high SBH conversion conditions. A reactor was designed and built as a part of a system to produce hydrogen from reaction (1) through the controlled addition of SBH fuel solutions to a supported catalyst. This system was thought to be multi-use. We chose a concentrated (19 wt %) SBH fuel solution because of its high gravimetric potential [8]. The fuel addition rate was selected to produce  $0.8\text{-}1.2 \text{ L} \cdot \text{min}^{-1}$  hydrogen. Temperatures of  $100\text{-}120^\circ\text{C}$  were achieved. The supported catalyst is a Co-B based material and it was prepared by chemical methods for the first time on bare and oxidized Stainless Steel (SS) home made monoliths searching for high adherence and contact with the fuel solution. Adherence was tested during 60 minutes-long-experiments. Durability of supported Co-B catalyst was tested by repeating the previous experiment for 11 cycles. Long life experiments were performed during 9 hours of hydrogen production. To compare the results a supported Ru-B catalyst was prepared for the first time on a previously oxidized SS monolith and durability was also tested during 11 cycles. Previously reported reactivation steps were used in this work when necessary and the effect of these steps assessed [7, 9].

Deactivation and reactivation is discussed herein in terms of formation, accumulation and elimination of B-O species, memory effect and nanoparticle growth.

## **2. Experimental**

### **2.1. The continuous system and the reactor**



For the experiments a home made system was designed and built [10]. Figure 1.a. shows a scheme of the system. It consists of a PP storage containing the stabilized fuel solution, which is connected with a commercial membrane pump. The cylindrical reactor is made of PMMA with a total volume of 11 mL (Fig.1.b). The reaction gas-liquid mixture flows from the reactor into a tank, which serves as a gas-liquid separator and in parallel provides a recipient volume for the residues. The hydrogen gas stream was further dried and purified by installing a 250 mL PP bottle filled with dry silica-gel. Hydrogen gas flow was measured by a flowmeter (Bronkhorst MassView MV-394-H2). The temperature at the exit of the reactor was measured by a thermocouple. The hydrogen generation rate (HGR) was constantly monitored as a function on time with the flowmeter connected to a PC. From the experiments, an (avgHGR $\pm$  error) (average Hydrogen Generation Rate) is obtained graphically from the HGR vs time plot, including the maximum fluctuations in the experimental error. The total conversion (TC %) was calculated as  $100 \times V/V_{th}$  where V represents the product between the avg HGR and the time (avgHGR x time) and  $V_{th}$  was calculated as the theoretical volume of hydrogen (at room temperature) to be obtained from the total volume of 19wt% fuel solution.

## **2.2. Support preparation**

As catalyst support homemade monoliths made from commercially available perforated stainless steel (SS316) were employed [10]. After washing in an ultrasound bath for 20 min using first deionised water and then 20 min using acetone to remove inorganic and organic impurities the thus obtained supports were weighted. The SS support was calcined at 900°C [10]. The adherence of the produced oxide layer was tested by immersing in an ultrasonic bath 20 minutes in deionized water and 20 minutes in acetone. The monolith was weighed before and after sonication and the loss of weight was calculated. No loss of the oxide layer was found for the calcined monolith.

## **2.3. Catalysts**

### **2.3.1 Catalysts preparation**

Two techniques were employed in this work and they are described as following:

i)  $\text{Co}_{\text{aq}}/\text{SBH}_{\text{aq}}$  technique has been used to prepare the Co-B catalyst on bare SS monoliths. The technique was used before and consists of 12 cycles of alternate immersions of the support on 30%  $\text{CoCl}_2 \cdot 6\text{H}_2\text{O}$  aqueous solution and on a stabilized 19 wt% SBH aqueous solution [8].

ii) The  $\text{Co}_{\text{ETOH}}$  or  $\text{Ru}_{\text{ETOH}}/\text{SBH}_{\text{aq}}$  technique similar to the one described in i) was employed to prepare the Co-B and Ru-B catalysts on previously oxidized SS monoliths. It is based on the use of ethanolic 30%  $\text{CoCl}_2 \cdot 6\text{H}_2\text{O}$  or  $\text{RuCl}_3 \cdot 3\text{H}_2\text{O}$  solutions as metal source [10]. After preparation, all samples were then treated at 573 K (heating rate  $1^\circ\text{C}/\text{min}$ ) in pure Helium environment for 2h before cooling to room temperature.

### **2.3.2 Catalysts characterization**

For characterization catalysts were also prepared on  $900^\circ\text{C}$  calcined 316 SS sheets (1cmx1cm). The sheets were also included in the reactor in all experiments and extracted for characterization. X-ray diffraction measurements were performed using  $\text{Cu K}\alpha$  radiation in a Siemens D5000 diffractometer in a Bragg-Brentano configuration in the  $2\theta$  angle range of 40-80 degrees.

Scanning electron microscopy (SEM) was performed to study the morphology of samples in a high resolution FEG microscope, HITACHI S4800.

### **2.3.3 Catalysts adherence and durability tests**

As it was desired to approach the study to real conditions, adherence and durability (upon cycles and in long term experiments) were tested in conditions of intense hydrogen bubbling at high temperatures.

The tests were conducted on the system described in 2.1 under a  $2.8\text{ml}\cdot\text{min}^{-1}$  constant flow of a fresh 19 wt % SBH solution stabilized in 4.5 wt % NaOH on the selected supported fresh catalyst. The fuel addition rate was selected to produce  $0.8\text{-}1.2\text{ L}\cdot\text{min}^{-1}$   $\text{H}_2$  which results in a temperature of  $100\text{-}120\text{ }^\circ\text{C}$ . The system was kept working during 60 min for the adherence and durability cycles tests and 9 hours during the long life tests. Then the fuel addition was interrupted. The reactor was allowed to reach room temperature, and then monoliths were extracted, washed with water and ethanol and dried under  $\text{N}_2$  flow.

The monoliths were weighted before and after operation and then the catalyst loss was calculated.

### **3. Results and Discussion**

#### **3.1. SS and oxidized SS support**

It is known that calcination of stainless steel produces an oxide layer that increases surface roughness and consequently the adhesion of catalysts [11-12]. For this reason Co-B catalyst was prepared using non-treated (bare) and oxidized SS monoliths [10]. Figure 2.a includes a SEM image of a non-treated SS monolith in comparison to a calcined SS monolith (Fig.2.b). Fig 2c. and 2.d. show the fresh Co-B prepared on both monoliths respectively. The surface roughness of the oxidized monolith induces a high degree of porosity at constant catalyst load ( in the range of  $10\text{-}14\text{ mg}_{\text{cat}}\text{g}_{\text{support}}^{-1}$  for bare and for the previously oxidized SS monolith). Adherence of Co-B catalyst supported on bare and oxidized SS monolith was 90% and 100% respectively (in both cases, tests conducted in duplicate). In the following sections Co-B catalyst will be supported on the previously oxidized monolith.

#### **3.2. Study of the reactor behaviour.**

The exothermic character of reaction (1) makes heat management a key issue. In this reactor the heat released in the reaction has to compensate heat losses due to heating-up of the fuel, heat transport out of the reactor by the reaction products and heat losses of the reactor to the surrounding. The heat production of the employed fuel and the chosen flow rate was sufficient to initiate and maintain the reaction. Figure 3.a. shows that for a selected fuel addition rate steady state with a constant HGR (avgHGR equal to  $0.9 \text{ L} \cdot \text{min}^{-1}$ ) and constant temperature ( $103^\circ\text{C}$ ) are obtained [10]. With this reactor it is possible to obtain stable hydrogen generation in the range of  $1.66\text{-}0.3 \text{ L} \cdot \text{min}^{-1}$  at constant temperatures (above the melting point of sodium borates) by varying the fuel addition rate [10]. For HGR lower than  $0.3 \text{ L} \cdot \text{min}^{-1}$  heat production is not sufficient to achieve appropriate temperature for the reactor maintain stable hydrogen generation. Lower HGRs would require an adapted reactor design.

When conducting durability experiments, a decrease in hydrogen generation rate could not only be attributed to a deactivation of the catalyst but also to the loss of catalyst during operation. To evaluate the effect of the amount of supported Co-B in the hydrogen generation rate, a series of previously calcined monoliths were prepared with variable catalyst amount. These catalysts were tested in the reactor at  $2.8 \text{ ml} \cdot \text{min}^{-1}$  fuel addition rate.

Figure 4 and table 1 show that Co-B load ( $\text{mg}_{\text{cat}} \cdot \text{g}_{\text{support}}^{-1}$ ) increases linearly with the number of coatings. The avg HGR responds sigmoidal to the mass of catalyst. With low catalyst amounts (7 mg) the reaction rate is not high enough to reach an appropriate temperature to self-maintain the hydrogen production. At 37 mg Co-B the reactor produces enough hydrogen and heat to achieve a  $0.8 \text{ L} \cdot \text{min}^{-1}$  hydrogen production at  $\sim 100^\circ \text{C}$ . An increase in the catalyst load does not cause significant variations in the hydrogen generation rate. This suggest that when the catalyst load is higher than 7mg hydrogen generation rate is determined by the fuel addition rate and not by catalytic

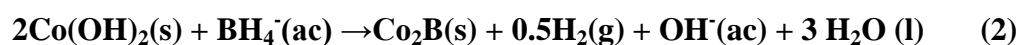
activity of the catalyst, except the deactivation achieves a degree that the reaction rate becomes catalyst-determined. The activity of the catalyst can be calculated as  $27 \text{ L}_{\text{hydrogen}} \cdot \text{min}^{-1} \cdot \text{g}_{\text{catalyst}}^{-1}$  which is between the highest ever reported activities for a non noble catalyst and means that oxidized monolith is a good dispersant [4].

This behaviour is useful when studying the deactivation process, since a significant reduction of the hydrogen generation rate can be definitely attributed to a deactivation process on condition that the catalyst loss is not high enough.

### 3.3. Durability of Co-B and Ru-B catalysts upon cycling

#### 3.3.1. Co-B catalyst

A fresh Co-B catalyst was tested in the continuous reactor at a  $2.8 \text{ ml min}^{-1}$  fuel addition rate during 60 min during 11 start-and-stop reuse cycles. Except for cycle 3, the reaction was initiated with a first addition of a small amount of fuel and waiting until the temperature reached at least  $60^\circ \text{ C}$ . This step represents an *in situ* reactivation (2) [8-9].



After 60 min of operation the reaction was interrupted, the monolith was washed with water and then with ethanol and dried at open air. After weighing of the monolith for the determination of catalyst losses the monolith was reused in additional 60 min cycles. The results of these experimental run are shown in Table 2. Figure 5.b represents the variation of the normalized avgHGR as a function of the number of cycle. A slight decrease of the normalized avg HGR was observed in the second cycle. However successive repetitions do not present any significant variations of the avgHGR until in cycle 7 a complete deactivation of the catalyst was observed. In this cycle at the beginning a slightly lower activity was observed, which dropped rapidly after ca. 10 min of reaction time to zero (Fig.5a). Repetition of this experiment confirmed this

result. In previous papers a layer of B-O based species on the catalyst surface were identified as being responsible of the deactivation of Co catalysts [7, 13]. Based on this assumption a reactivation step was applied, which consisted in washing with diluted acid solution to eliminate B-O based compounds on the surface similarly to reference [7]. After this reactivation step the avgHGR recovered in the subsequent cycles 9, 10 and 11. Nevertheless even by acidic treatment the avgHGR did not reach fully the initial value ( $\text{avgHGR}_0$ ), which indicates that more stable and resistant B-O based species were formed and/or that some more profound change of the catalyst has taken place. Figure 6 shows SEM micrographs for the fresh Co-B catalyst (6.a-b) in comparison to the catalyst before reactivation (6.c-d) and the diluted acid reactivated (5.f-g) Co-B. The fresh catalyst (Fig.6.a) is very porous and higher magnification micrographs clearly show the formation of spherical nanoparticles (Fig.6.b). Fig 6.c. shows the catalyst before acid reactivation. It seems to have lost porosity and dispersion, which could indicate a deposition of B-O based species on the catalyst surface. High magnification (Fig.6.d.) shows the same layer that was previously recognized as the B-O based deactivating network [7]. After diluted acid reactivation, the structure of the catalyst seems to be recovered from a textural point of view (Fig.6.f.), but porosity is still lower than in the case of the fresh catalyst (Fig.6.a.). This could explain that the activity is recovered after diluted acid treatment but not to the same extent than in the 1-6 cycles. It seems that B-O based species are formed on the catalyst surface, which could not be removed fully by diluted acid treatment but remain partially. Higher magnification (6.g.) supports this assumption showing that the nanoparticles are accessible again but part of the catalyst is still covered by the B-O species' layer.

Except for cycle 3 adherence of the catalyst during the 11 cycles was found to be as high on condition that the *in situ* reactivation was performed. Neither visible loss of catalyst was observed nor was Co-B powder found in the residual tank.

### **3.3.2. Supported Ru-B as catalyst**

Previous studies suggested that Ru based catalysts could be more stable against deactivation [14, 15]. To prove this we prepared a Ru-B catalyst on a previously oxidized monolith and we tested it upon cycling in the same conditions than the Co-B catalyst [10]. In the first 7 cycles we found a behaviour similar to that of the Co-B catalyst (section 3.3.1). During the first three cycles the avgHGR of the Ru-B remained constant. In the following cycles 4-6 a slight drop of avgHGR was observed (90% of avgHGR retained in respect to the initial) until in cycle 7 a complete deactivation occurred (Fig.7). Diluted acid washing as reactivation step permits to recover the avgHGR in a single cycle but in subsequent cycles deactivation again is observed. After a second reactivation avgHGR diminished to a 60% in respect to the initial and finally deactivated completely for a third time. Figure 8.a. shows a representative SEM image of the fresh Ru-B catalyst in comparison to the deactivated catalyst (Fig.8.b.) after 11 cycles. In this case B-O based species' formation seems not to be the critical effect but evidence of particle aggregation is found in SEM images of the deactivated catalyst. On the other hand the catalyst treated with diluted acid showed in studies by SEM no microstructural difference in respect to the deactivated one despite avgHGR is partly recovered. This supports the assumption that deactivation is depending on formation of B-O based compounds on one side and on the other side on particle agglomeration but in this case the latter is the determining effect.

### **3.4. Durability of the Co-B catalyst in a long-life experiment.**

A long time continuous experiment (9h) was conducted on a fresh Co-B catalyst on oxidized SS monolith. Stable hydrogen generation at the same HGR was obtained during 4 hours and then HGR decreased slowly to reach 90% of the initial at the end of

the experiment (Figure 9). The catalyst is clearly more durable in a single long time experiment than upon start-stop cycling. SEM micrographs of the fresh Co-B catalyst (Fig. 10.a-b) in comparison to the 9h used Co-B (Fig. 10.c-d) show that the formation of B-O compounds is here not occurring and no evidence of particle aggregation is found. The catalyst used continuously of 9 hours is as disperse and porous as the fresh. XRD measurements show that the continuously used catalyst presents a broad peak between 20-45 2θ degrees with some sharp peaks which were identified as coming from a Na<sub>2</sub>B<sub>4</sub>O<sub>7</sub> layer (Fig 11, indicated by arrows) . Adherence of the Co-B catalyst was higher for the 9h experiment than for the 9 cycle experiments.

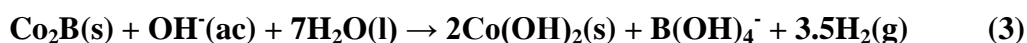
Diluted acid washing was successful in removing this Na<sub>2</sub>B<sub>4</sub>O<sub>7</sub> layer but also is aggressive with the catalyst because it destroys its adherence. It is concluded that the formation of B-O based compounds network could be the responsible of the 10% loss of avgHGR respect to the initial.

Based on these observations it can be concluded that the formation of borates on the catalyst surface, which is responsible for the loss of activity and adherence together with the intense hydrogen formation of the catalytic layer, mostly is occurring during the start or stop operations. On the other side the conditions under which the reaction is taking place inside the reactor is mostly inhibiting this formation of B-O species on the catalyst surface and are extending largely the life time and stability of the supported catalyst.

### **3.5. Deactivation, reactivation step and memory effect.**

Three deactivation mechanisms of the catalyst for reaction (1) have been reported [4,7, 9, 13]

- i) Oxidation of the Co catalyst at the end of the reaction as suggested in equation (3) [9].





- ii) Accumulation of B-O and (Na,Co) based compounds on the catalyst surface [7,13]
- iii) Agglomeration of particles [13].

The strong alkaline medium also favours catalysts deactivation and this effect cannot be disregarded.

Deactivation by mechanism i) should be recovered by a treatment with a reducing agent, which in our case is the fuel solution itself. The *in situ* treatment applied in our work was able to recover the catalytic activity of the Co-B and the Ru-B catalyst at least partially. A washing of the catalyst with a diluted acidic solution is expected to be efficient against deactivation by mechanism ii). The *ex situ* reactivation by acidic solution showed mostly good results in the case of the Co-B catalyst upon cycling, in which SEM has shown a strong B-O based compounds formation (Fig 7 c-d). In the case of the Ru-B catalyst a much lower B-O species formation was observed, but also *in situ* and *ex situ* reactivations proved to be much less efficient. In this case a deactivation by particle aggregation according to mechanism iii) seems to take place (Fig 9).

Long life of the Co-B catalyst is affected mainly by B-O species formation and no aggregation was found. In this case B-O species based network is not as strong as in cycling experiments which explains the high durability and no deactivation after 6 h use. The start-stop, washing, cooling and storing of the catalyst seems to stabilize the B-O species' layer with a higher deactivation effect. Because of the sigmoid reactor behaviour (section 3.2.) B-O based compounds' accumulation does not produce a significant effect until the catalyst surface is highly covered. *Ex situ* diluted acid reactivation was not completely effective and is negative for catalyst adherence. On the contrary, high temperature reaction and B-O based compounds' elimination in the continuous system makes the catalyst more durable on long experiments.

Very recently it was reported the absorption of small amounts of hydrogen on catalysts during preparation processes [16]. This may result in metal catalyst pulverization due to the effect of lattice expansion. Despite it should be further studied, this effect cannot be disregarded in herein presented experiments, not only during catalyst preparation but also during each start-stop cycle.

#### **4. Conclusions**

The intention of this work was to explore the performance of a Co-B catalyst for the production of hydrogen by SBH hydrolysis under conditions of a practical use. This included a continuous long time use of the catalyst and a high throughput of SBH to achieve a high hydrogen production rate. For this purpose a system was designed including a continuous reactor and the catalyst supported on a SS monolith. To the best of our knowledge it is the first time that a Co-B catalyst is prepared on a previously calcined SS monolith, which has proven to be a good catalyst dispersant, cheap and adherent enough to conduct cycling and long time experiments. Special interest was laid on long time durability of the catalyst and on possibilities to regenerate the catalyst in order to recover its activity. In long time experiments the continuous system showed the possibility of using the synergies between operational temperature and continuous elimination of borates formed in the reaction. A certain deactivation of the catalyst was observed. Two kinds of reactivation techniques were applied, an *in situ* reactivation step consisting in a pre-treatment by SBH and an *ex situ* step by washing with a diluted acid solution, which were able to restore mostly the catalyst activity. Nevertheless, a deactivation after several cycles in a start-stop operational mode could be observed, which proved to be resistant to intents of regeneration. This memory effect can be related to the formation of a network B-O based compounds on the Co-B surface. Co-B particle aggregation seems not to be a major deactivation process neither for long time

continuous nor for cycling experiments. In the case of and Ru-B catalyst particle agglomeration seems to be the major deactivation process but the formation of surface borates cannot be disregarded.

M-B chemistry is put in evidence here. In the case of the Co-B material metal metalloids interactions, which are highly stabilizing particles against agglomeration, B-O adsorption is higher but reversible upon acid washing [15-17]. In the case of the Ru-B material the low affinity of ruthenium to boron makes the catalyst more susceptible to particle agglomeration and prevents B-O adsorption making washing with acids less effective [15]. The study of particle aggregation will be conducted in a further study through TEM (Transmission Electron Microscopy) and HREM (High Resolution Electron Microscopy).

In this work was demonstrated that in practical uses for a high rate Hydrogen production non noble catalysts like Co are presenting very good and cheap alternatives to noble metal catalysts.

### **Acknowledgements**

Financial support from Abengoa Hidrógeno S.A., MICINN (Project CTQ2009-13440), “Junta de Andalucía” (TEP217) and the EC (CT-REGPOT-2011-1-285895, AL-NANOFUNC) is acknowledged.

We thank to Dr. Angel Justo for the XRD measurements.



## 5. References

- [1] B.H. Liu, Z.P. Li. A review: Hydrogen generation from borohydride hydrolysis reaction. *J. Power Sources*, 2009; 187: 527-534. References therein
- [2] U.B Demirci, O.Akdim, J. Andrieux, J. Hannauer, R. Chamoun, P.Miele. Sodium borohydride hydrolysis as hydrogen generator: Issues, state of the art and applicability upstream from a Fuel Cell. *Fuel Cells*, 2010; 3: 335-350. References therein
- [3] H.I. Schlesinger, H.C. Brown, A.E. Finholt, J.R. Gilbreath, H.R. Hoekstra, E.K. Hyde. Sodium borohydride, its hydrolysis and its use as a reducing agent and in the generation of hydrogen. *J. Am. Chem. Soc.*, 1953; 75: 215-219.
- [4] S.S. Muir, X. Yao, Progress in sodium borohydride as a hydrogen storage material: Development of hydrolysis catalysts and reaction systems. *Int J. Hydrogen Energy*, 2011; 36: 5983-5997. References therein
- [5] U.B. Demirci, P.Miele, Cobalt in  $\text{NaBH}_4$  hydrolysis. *Phys. Chem. Chem Phys*, 2010; 12: 14665-14651. References therein
- [6] U.B. Demirci, O. Akdim, J. Hannauer, R. Chaumoun, P. Miele. Cobalt, a reactive metal in releasing hydrogen from sodium borohydride by hydrolysis: A short review and a research perspective. *Sci China Chem*, 2010; 53: 1870-1879.
- [7] O.Akdim, U.B. Demirci, P. Miele, Deactivation and reactivation of cobalt in hydrolysis of sodium borohydride. *Int. J. Hydrogen Energy*, 2011; 36: 13669-13675.
- [8] G.M. Arzac, A. Fernández, A. Justo, B. Sarmiento, M.A. Jiménez, M.M. Jiménez. Optimized hydrogen generation in a semicontinuos sodium borohydride hydrolysis reactor for a 60-W scale fuel cell stack. *Journal of Power Sources*, 2011; 196: 4388-4395
- [9] A. Garron, D. Świerczyński, S. Bennici, A. Auroux. New insights into the mechanism of  $\text{H}_2$  generation through  $\text{NaBH}_4$  hydrolysis on Co-based nanocatalysts

studied by differential reaction calorimetry. *Int. J. Hydrogen Energy*, 2009; 34: 1185-1199.

[10] G.M. Arzac, D. Hufschmidt, E Jiménez Roca, A. Fernández, M.A. Jiménez, S. Tyagi, M.M. Jiménez, B. Sarmiento. "Proceso de producción de hidrógeno mediante hidrólisis catalítica en un reactor continuo para llevar a cabo dicho procedimiento". Spanish patent application: P201230221. Priority date: 14-Feb-2012. Presented by Abengoa Hidrógeno S.A.

[11] J.P. Bortolozzi, E.D. Banús, V.G. Milt, L.B. Gutierrez, M.A. Ulla. The significance of passivation treatments on AISI 314 foam pieces to be used as substrates for catalytic applications. *App. Surf. Sci*, 2010; 257: 495-502.

[12] P. Avila, M. Montes, E.E. Miró, Monolithic reactors for environmental applications A review on preparation technologies. *Chem. Eng. Journal*, 2005; 109: 11-36.

[13] J.H. Kim, K.T. Kim, Y.M. Kang, H.S. Kim, M.S. Song, Y.J.Lee, P.S.Lee, J.Y. Lee, Study on degradation of filamentary Ni catalyst on hydrolysis of sodium borohydride. *J.Alloys and Compds.*, 2004; 379: 222-227.

[14] U.B. Demirci, F. Garin, Ru-based bimetallic alloys for hydrogen generation by hydrolysis of sodium tetrahydroborate, *J. Alloys and Compds*, 2008; 463: 101-111

[15] G.M. Arzac, T.C. Rojas, A. Fernández, New insights into the synergistic effect in bimetallic-boron catalysts for hydrogen generation: The Co-Ru-B system as a case study. <http://dx.doi.org/10.1016/j.apcatb.2012.02.013>

[16]H.B. Dai, Y. Liang, P. Wang, Effect of trapped hydrogen on the induction period of cobalt-tungsten-boron/nickel foam catalyst in catalytic hydrolysis reaction of sodium borohydride. *Catalysis Today*, 2011; 170, 27-32.

[17] G.M. Arzac, T.C. Rojas, A. Fernández, Boron compounds as stabilizers of a complex microstructure in a Co-B catalyst for NaBH<sub>4</sub> hydrolysis. *Chem Cat Chem*, 2011; 3: 1305-1313.



## Figure captions

**Figure 1.** (a) Scheme of the home made system: (1) fuel tank, (2) pump, (3) continuous reactor (4) separation tank (5) drying system (6) flowmeter and (7) thermocouple  
(b) Scheme of the continuous reactor.

**Figure 2.** SEM micrographs of the SS. Monolith (a) before and (b) after calcination at 900°C. SEM micrographs of the fresh Co-B catalyst prepared on (c) bare SS monolith and on a (d) 900° C calcined SS monolith.

**Figure 3.** (a) Hydrogen Generation Rate and temperature as a function of time for 2.8ml.min<sup>-1</sup> fuel addition rate on a fresh Co-B catalyst.

**Figure 4.** Average Hydrogen Generation Rate under fixed fuel addition rate in employing the continuous reactor and Co-B catalyst load as a function of the number of coatings.

**Figure 5.** (a) Hydrogen Generation Rate as a function of time for the first, the seventh and the ninth (after diluted acid reactivation) cycle on the same Co-B supported catalyst.  
(b) Catalytic activity represented by the normalized rate ( $\text{avgHGR}/\text{avgHGR}_0$  where  $\text{avgHGR}_0$  represents the average HGR for cycle 1) as a function of the cycle number for the cycling experiments on supported Co-B catalyst.

**Figure 6.** SEM micrographs at two different magnifications of the Co-B catalyst upon cycling at different stages: (a-b) Fresh catalyst (c-d) the Co-B catalyst used 8 times; before diluted acid reactivation ; (f-g) the Co-B catalyst after diluted acid reactivation.

**Figure 7.** Catalytic activity represented by the normalized rate ( $\text{avgHGR}/\text{avgHGR}_0$ , where  $\text{avgHGR}_0$  represents the average HGR for cycle 1) as a function of the cycle number for the supported Ru-B catalyst for the start-stop experiments.



**Figure 8.** SEM micrographs of the **(a)** fresh and **(b)** the deactivated ( after 11 cycles) Ru-B supported catalyst.

**Figure 9.** Hydrogen Generation Rate as a function of time for the 9h long life test on a fresh supported Co-B catalyst.

**Figure 10.** SEM micrographs of the fresh **(a-b)** and the 9h continuously used **(c-d)** Co-B catalyst.

**Figure 11.** XRD of the fresh Co-B catalyst in comparison to the 9h continuously used after and before diluted acid reactivation. The substrate diffractogram is also included.

## Table Legends

**Table 1.** Average HGR and catalyst load as a function of the number of Co-B coatings.

**Table 2.** Experimental parameters for the 11 cycle experiment on the Co-B catalyst.

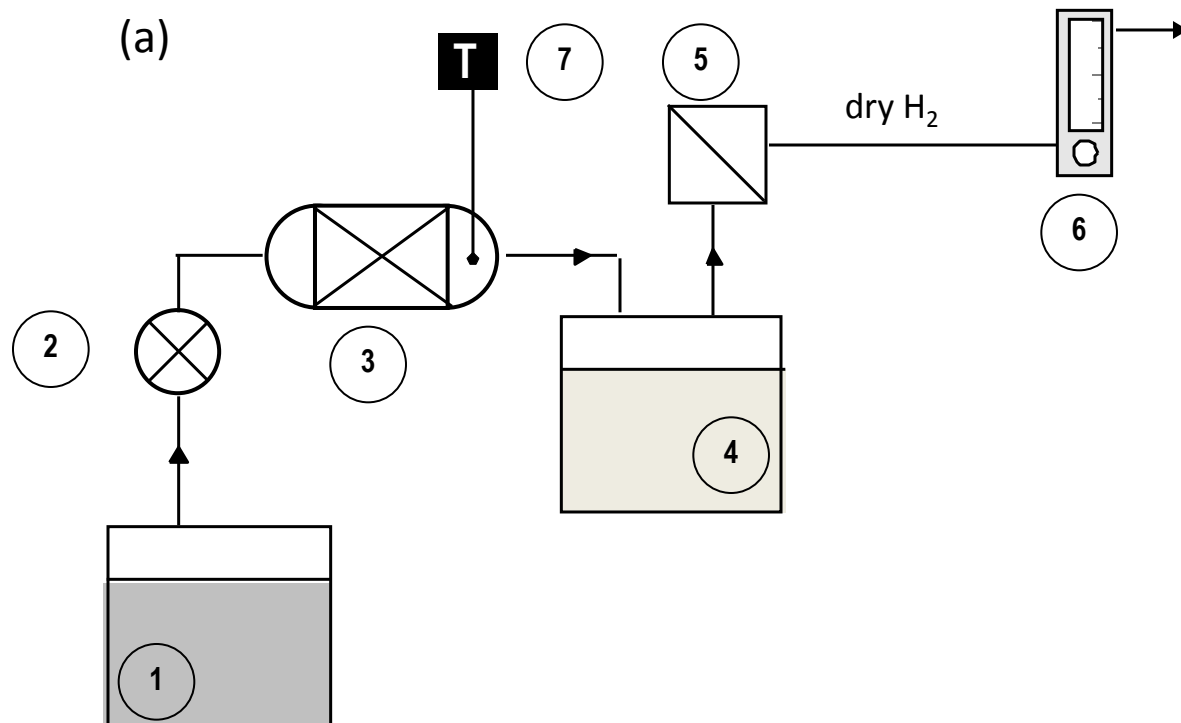
TABLE 1

<b>Number of coatings</b>	<b>Co-B load (<math>m_{\text{gcat}} \cdot g_{\text{support}}^{-1}</math>)</b>	<b>Co-B mass (mg)</b>	<b>Avg HGR (<math>L \cdot \text{min}^{-1}</math>)</b>	<b>TC (%)</b>
<b>0</b>	<b>0</b>	<b>0</b>	<b>0</b>	<b>0</b>
<b>2</b>	<b>1.34</b>	<b>7</b>	<b>0</b>	<b>0</b>
<b>4</b>	<b>7</b>	<b>37</b>	<b><math>0.87 \pm 0.05</math></b>	<b>62</b>
<b>6</b>	<b>12</b>	<b>65</b>	<b><math>0.89 \pm 0.05</math></b>	<b>64</b>
<b>8</b>	<b>23</b>	<b>126</b>	<b><math>0.90 \pm 0.05</math></b>	<b>64</b>
<b>10</b>	<b>32</b>	<b>182</b>	<b><math>1 \pm 0.06</math></b>	<b>71</b>
<b>12</b>	<b>33</b>	<b>202</b>	<b><math>0.85 \pm 0.06</math></b>	<b>61</b>

TABLE 2

<b>Cycle number</b>	<b>Co-B Mass loss (mg)</b>	<b>Avg HGR (L.min<sup>-1</sup>)</b>	<b>TC (%)</b>
1	<b>7.3</b>	0.87±0.02	62
2	0	0.74±0.03	53
3	<b>20</b>	0.85±0.04	61
4	0	0.87±0.03	62
5	0	0.81±0.04	58
6	0	0.87±0.03	62
7	0	From 0.5 decreasing to zero	--
8	0	0	--
9	0	0.7±0.02	50
10	<b>7</b>	0.74±0.03	53
11	<b>1.5</b>	0.74±0.02	53

Figure



(b)

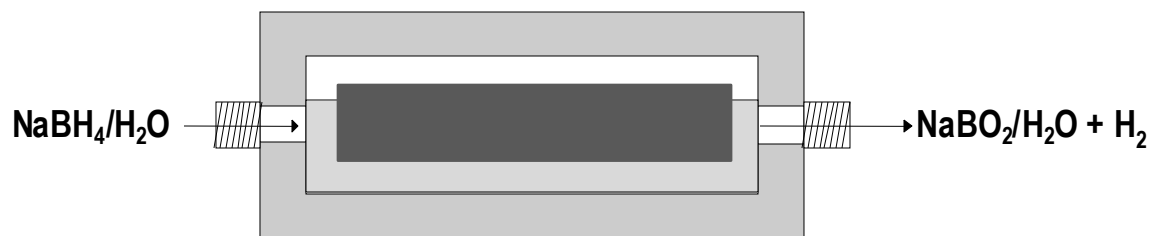


Figure 1.

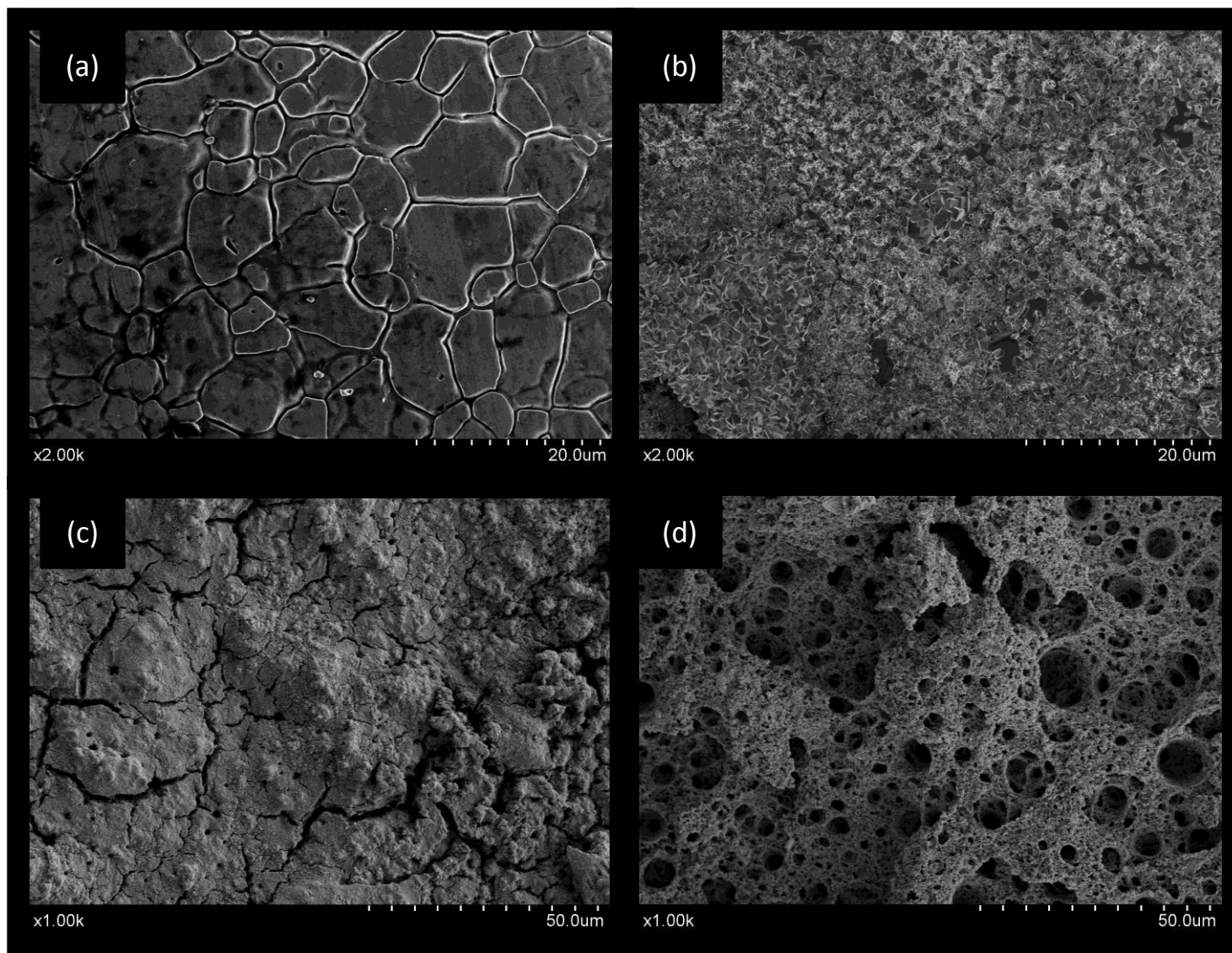
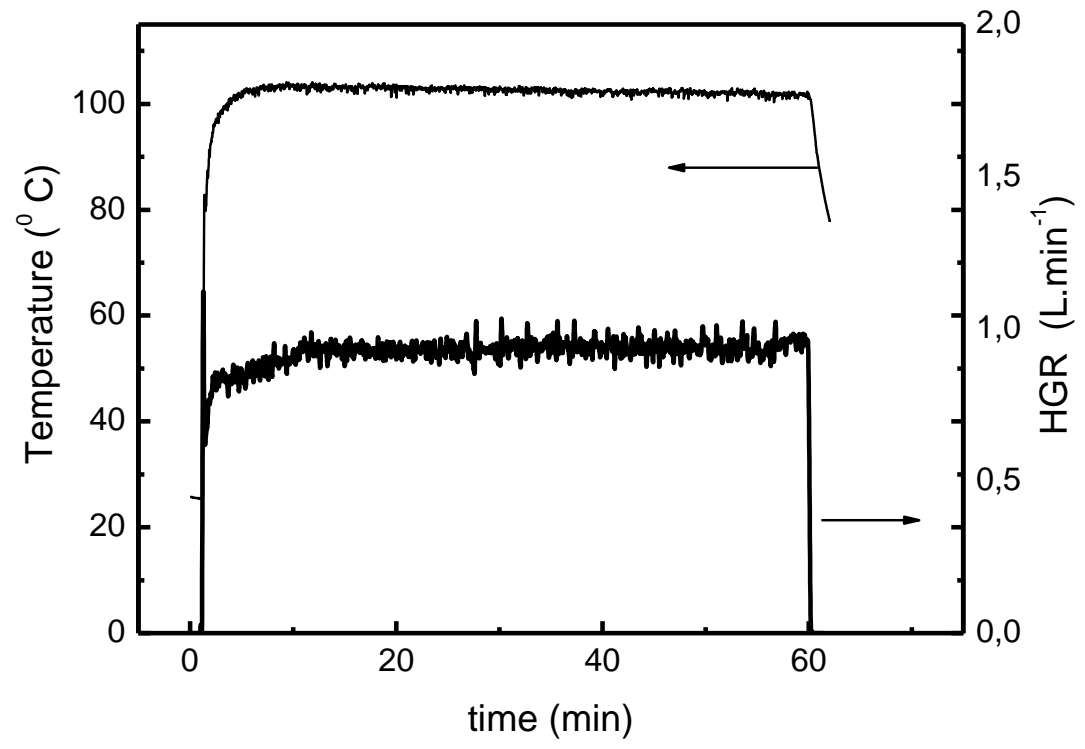
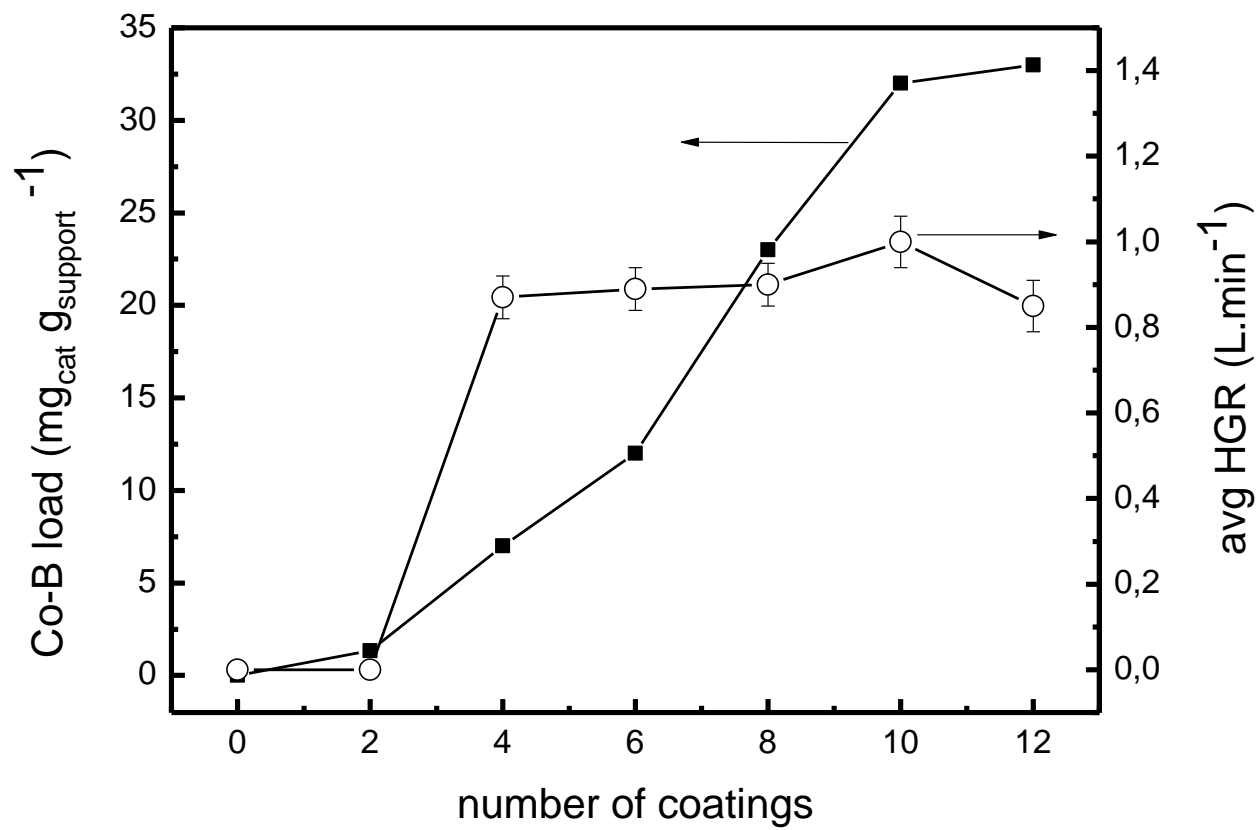


Figure 2

Figure 3







Figure

FIGURE 5

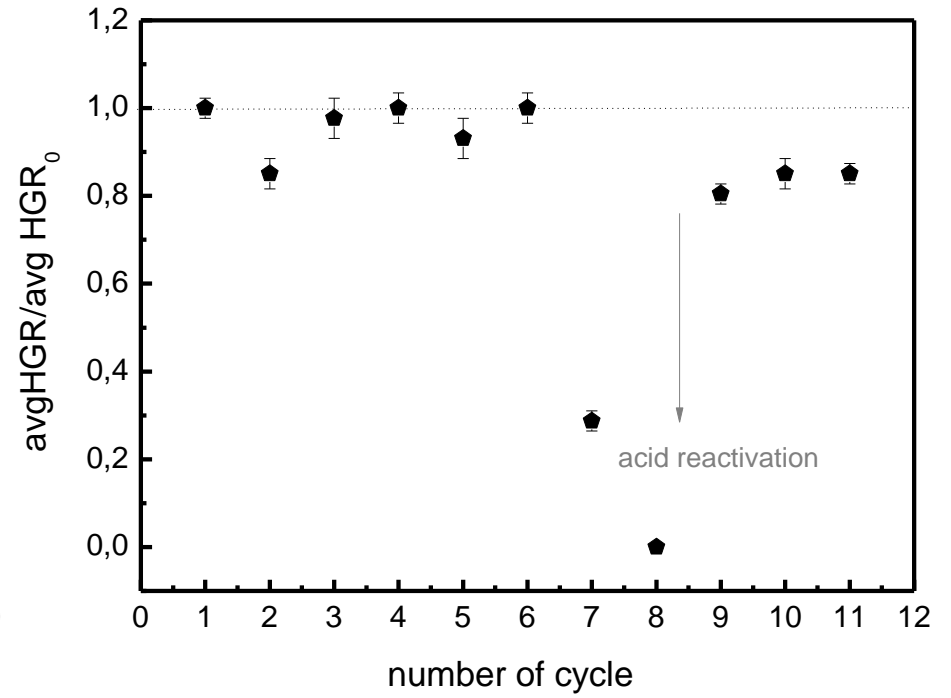
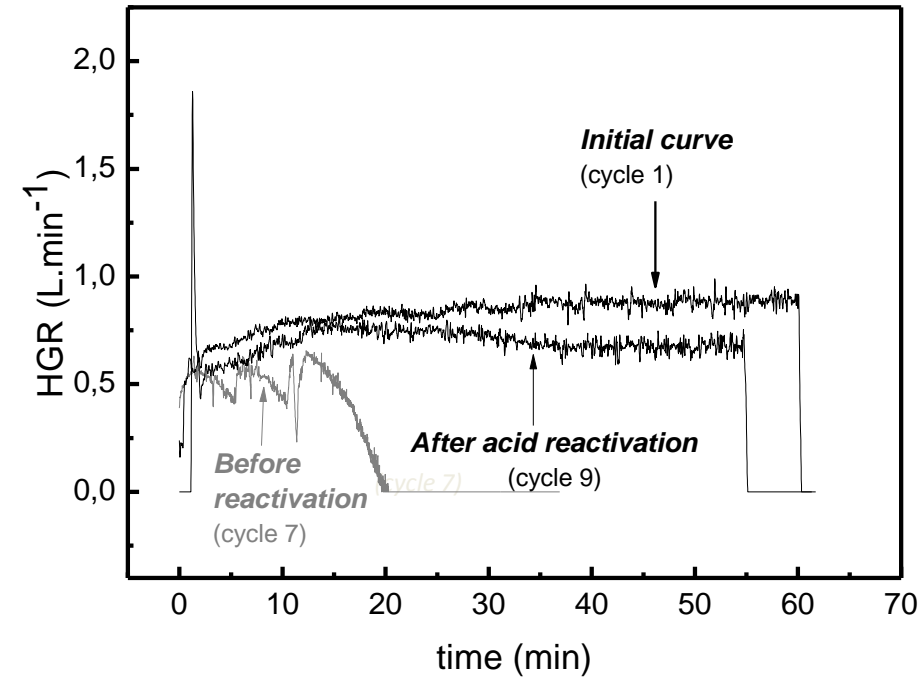


# FIGURE 6

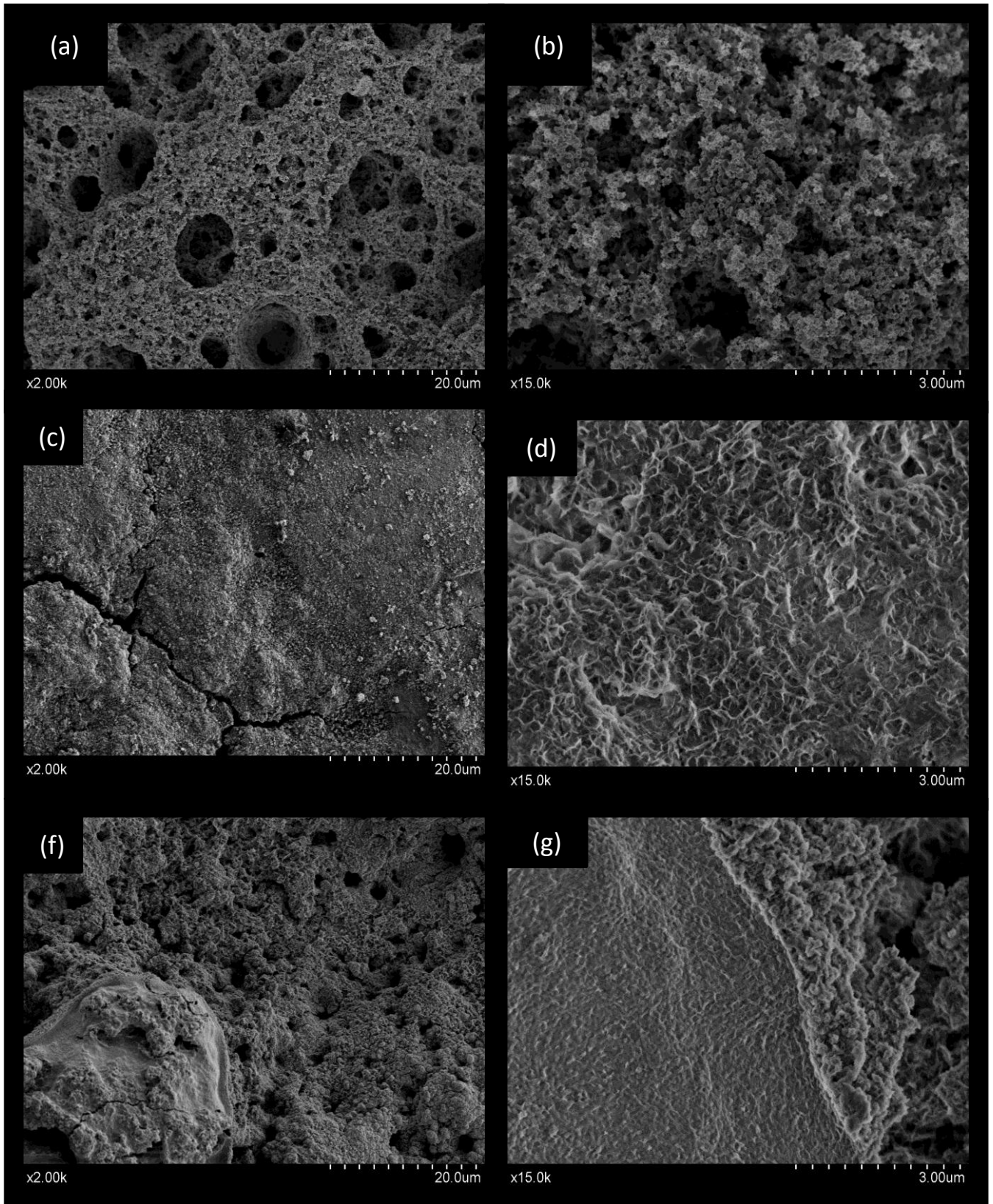


Figure 7

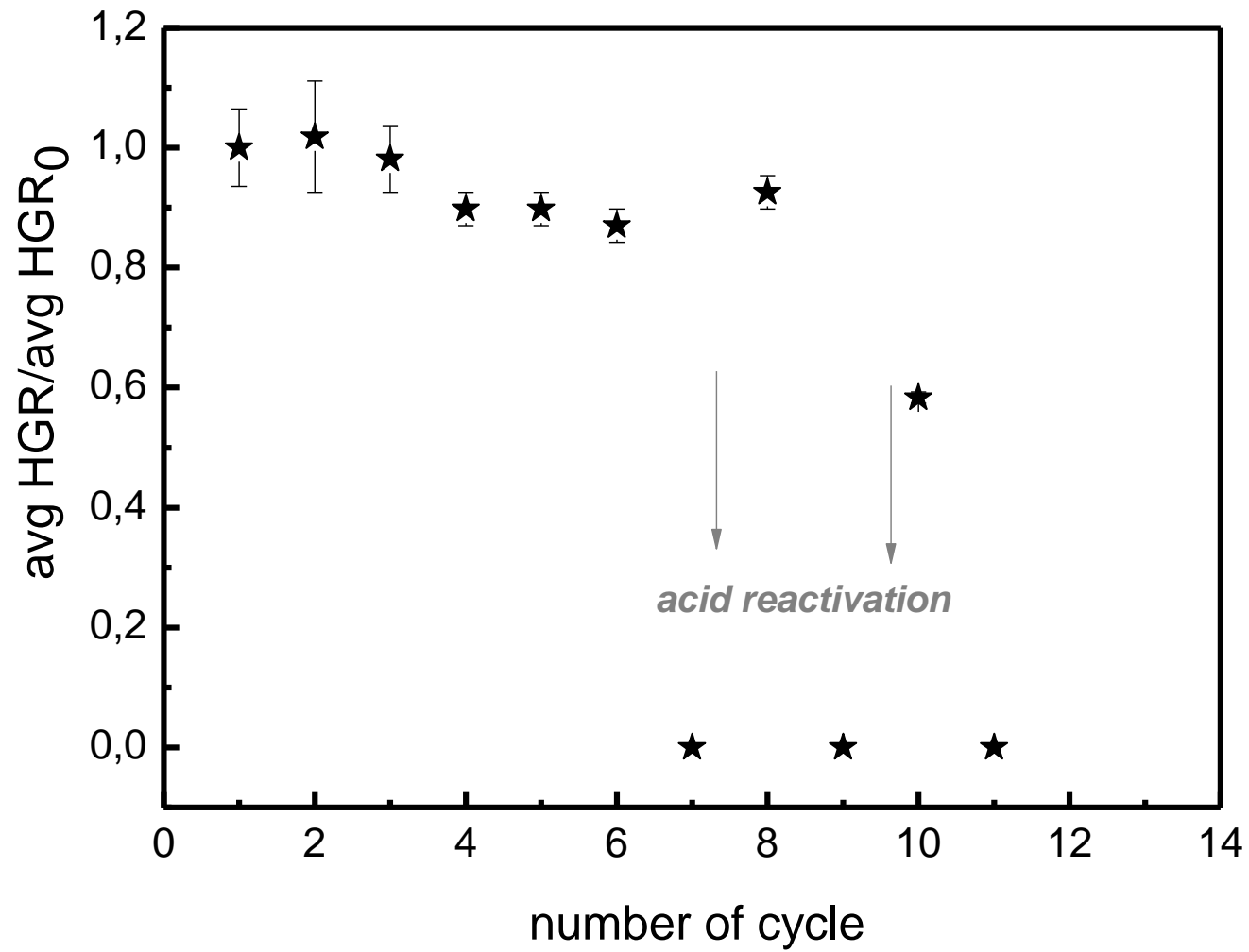


Figure 8

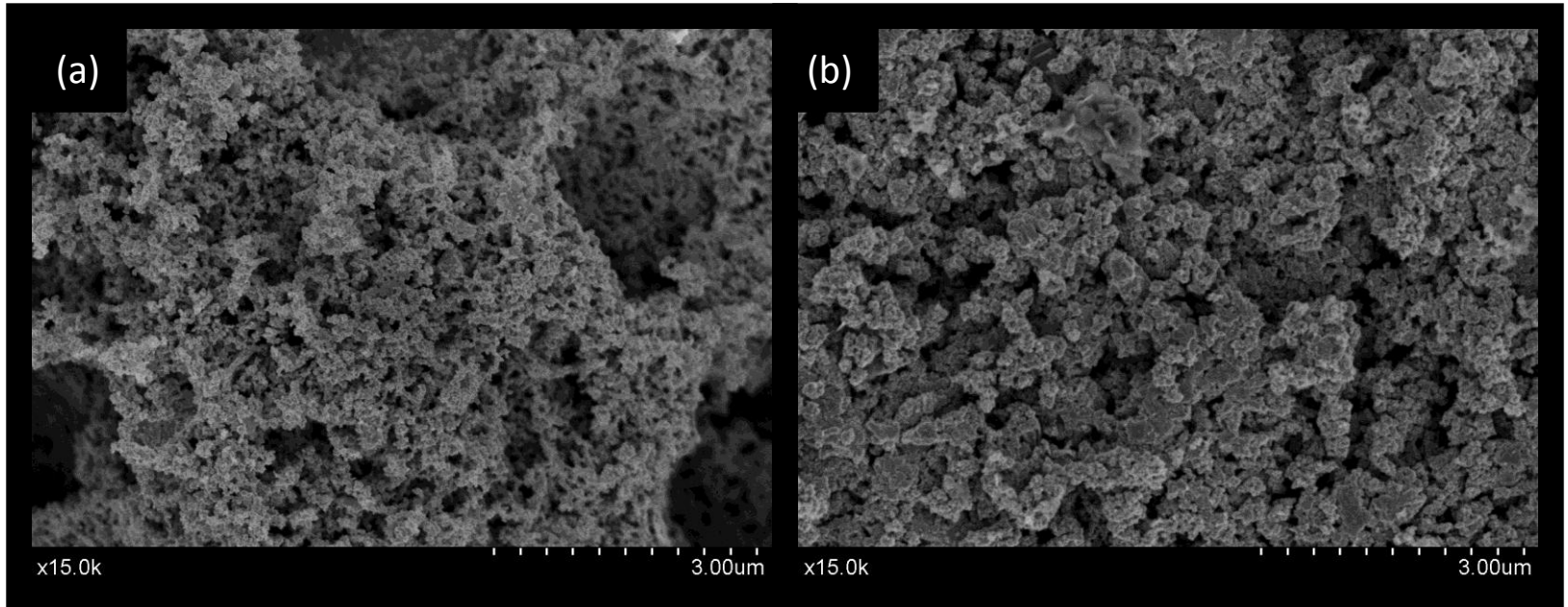


Figure 9

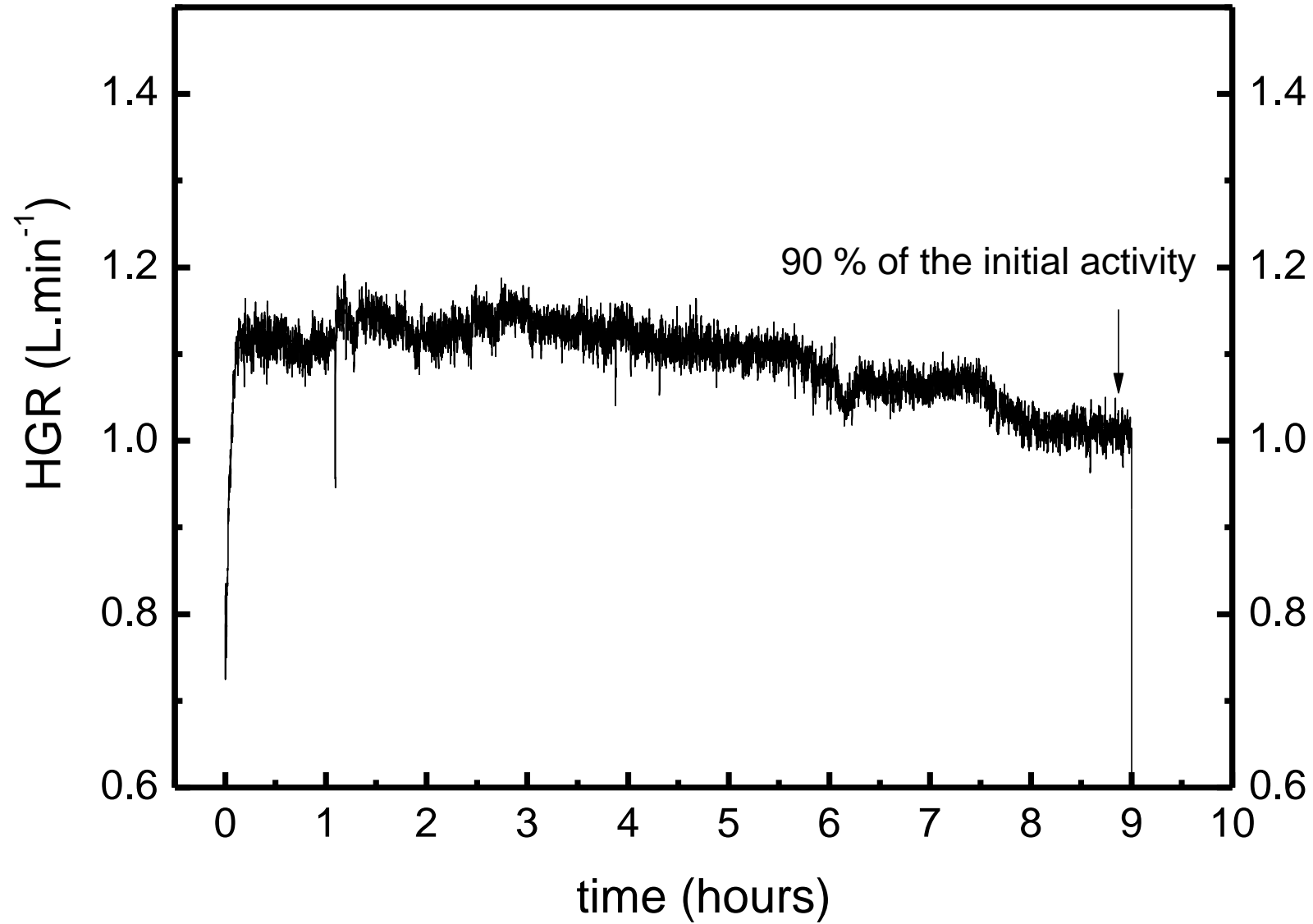


Figure 10

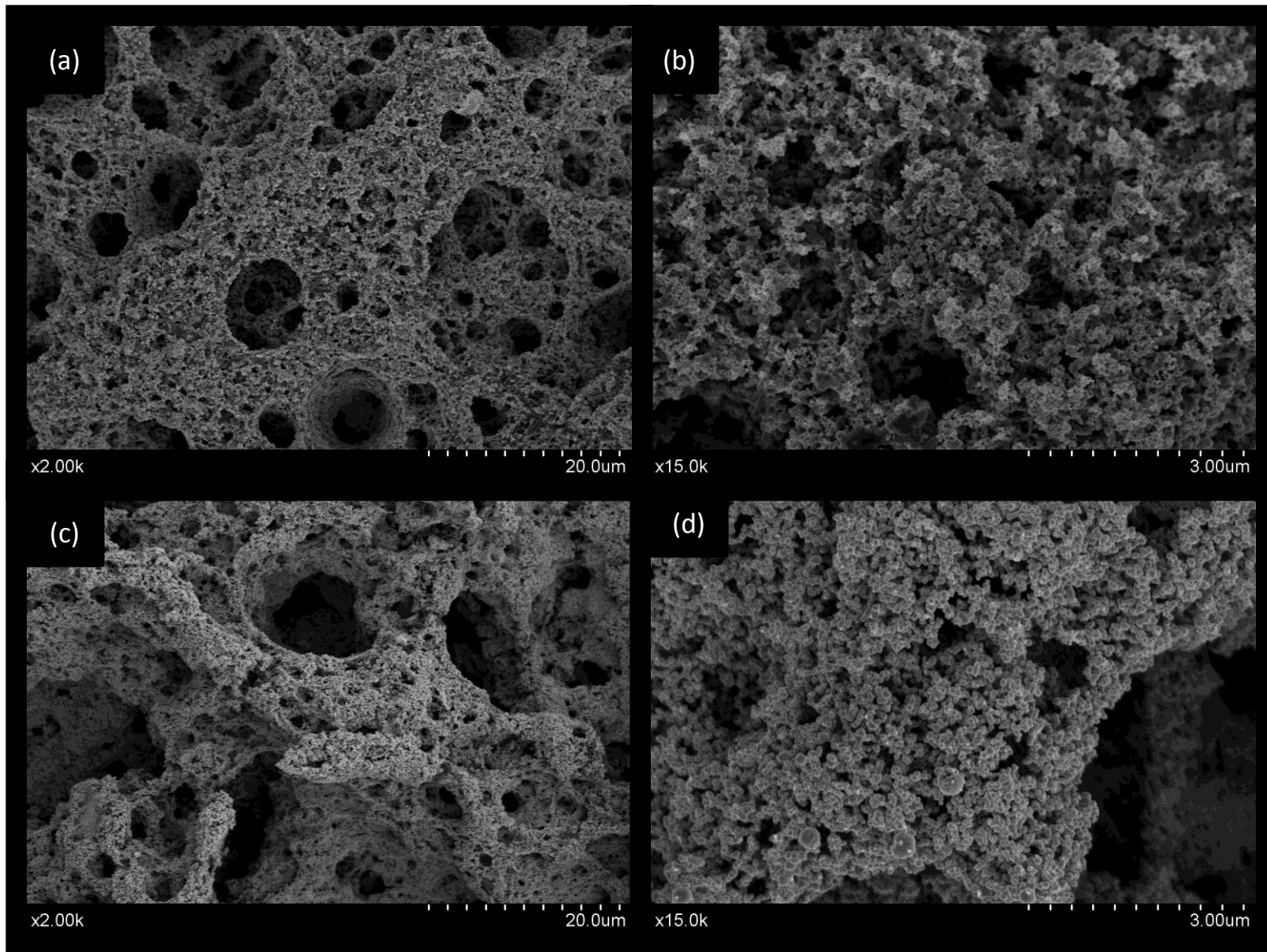


Figure 11

